Phase Separation and Crystallization Phenomena in a Poly(ester–carbonate) Block Copolymer: A Real-Time Dielectric Spectroscopic and X-ray Scattering Study

T. A. Ezquerra,*,† Z. Roslaniec,†,§ E. López-Cabarcos,‡ and F. J. Baltà-Calleja†

Instituto de Estructura de la Materia, C.S.I.C., Serrano 119, Madrid 28006, Spain, and Facultad de Farmacia, Universidad Complutense de Madrid, Madrid 28040, Spain

Received February 10, 1995; Revised Manuscript Received April 4, 1995[⊗]

ABSTRACT: The change of the relaxation process associated with the long-range motions during crystallization of an amorphous poly(butylene terephthalate)–polycarbonate block copolymer (PBT–PC) has been followed in real time by means of measurement of the dielectric complex permittivity. The observed decrease of the dielectric strength has been correlated to the appearance of crystallinity as detected by real-time wide- and small-angle X-ray scattering experiments using synchrotron radiation. The phenomenological Havriliak–Negami description has been used to analyze the changes of the dielectric strength, central relaxation time, and shape parameters describing the relaxation as crystallization proceeds. The influence of the crystalline lamellae on the dynamics of the amorphous phase for the PBT–PC(60/40) thermoplastic elastomer has been examined and compared with the relaxation processes of related homopolymers. The differences obtained are discussed by considering that PBT block copolymers typically crystallize by formation of spherulitic superstructures in which the degree of crystallinity is smaller than in those formed by homopolymers. Finally, phase separation in the early stages of crystallization has been discussed on the basis of Cahn's linearized theory of spinodal decomposition.

1. Introduction

It is well known that the combination of chemically distinct species in a block copolymer notably influences the physical properties of the resulting material.[1] The phase behavior of block copolymers is controlled by two factors: (a) polymerization stoichiometry, which determines both the concentration of each copolymer (f) and the degree of polymerization (N), and (b) the Flory–Huggins interaction parameter (χ) of the two components which form the block copolymer.[2] Depending on the values of the product χN and of the parameter f, block copolymers may suffer a transition from a disordered state in which both components are mixed to a locally segregated state in which microdomains rich in each component appear.[2,3] In addition, block crystallization can also occur in particular cases.[4]

Thermoplastic elastomers are block copolymers typically composed of "soft" segments, characterized by a low glass transition temperature, and "hard" segments having high strength and high melting temperatures.[1,5–8] The ability of the hard segments to crystallize leads to the appearance of crystalline hard segment rich domains.[1] The resulting semicrystalline copolymers exhibit combined properties of vulcanized rubbers and plastics. Both kinetics and phase separation mechanisms control the final properties of the copolymers.

Block copolymers based on poly(butylene terephthalate) (PBT) and polycarbonate (PC) exhibit a higher melting point depression, due to the presence of PC blocks, than typical poly(ester–ether) block copolymers like those based on PBT and poly(tetramethylene oxide) (PO4).[5,9,10] They also present lower crystallinity values.[11] This is so because the Flory–Huggins interaction parameter for PBT–PC is expected to be lower than for PBT–PO4 on the basis of the solubility parameters.[7] The interaction between the hard and soft segments slows down the kinetics of crystallization, depending on the hard-segment concentration. This makes these systems suitable candidates to investigate and differentiate the mechanisms of phase separation and crystallization.

Measurements of the dielectric relaxation associated with the long-range motions occurring above the glass transition temperature (T_g) can be used to characterize the changes occurring in glassy polymers during isothermal crystallization processes.[12–14] The changes observed in the parameters describing the shape of the dielectric relaxation during crystallization have been interpreted as being due to the restriction in the long-scale motions of the polymeric chains as the material is filled in with crystals.[15]

The Havriliak–Negami relaxation function has been shown to be very useful to characterize relaxation processes.[16,17] The Havriliak–Negami formulation proposes a frequency dependence of the complex dielectric permittivity for a system with a fast subglass relaxation (f) and a slow relaxation (s) of the form[15,16]

$$\epsilon^* = (\Delta\epsilon^*)_s + (\Delta\epsilon^*)_f + (\epsilon_\infty)_f \tag{1}$$

with

$$\Delta\epsilon^* = \frac{\epsilon_0 - \epsilon_\infty}{[1 + (i\omega\tau_0)^b]^c} \tag{2}$$

where ϵ_0 and ϵ_∞ are the relaxed and unrelaxed dielectric constant values, τ_0 is the central relaxation time, and b and c are the shape parameters which describe the symmetric and the asymmetric broadening of the relaxation time distribution function, respectively.[16] Schönhals and Schlosser proposed a model[18] in which the shape parameters can be related to the molecular dynamics at the glass transition provided that the molecular mobility is controlled by inter- and intramo-

† Instituto de Estructura de la Materia, C.S.I.C.
‡ Universidad Complutense de Madrid.
§ Permanent address: Institute of Materials Engineering, Technical University of Szczecin, Al. Piastow 17, 70-310 Szczecin, Poland.
⊗ Abstract published in *Advance ACS Abstracts,* May 15, 1995.

0024-9297/95/2228-4516$09.00/0

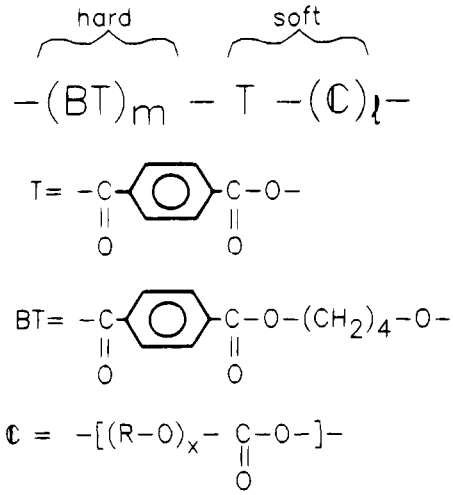

Figure 1. Schematics of the investigated copolymer. $m \approx 11$, $l \approx 10$, and $x \approx 1.12$; R = C_6H_{12} isomers. The given data are average values derived from stoichiometric ratio and NMR analysis.

lecular interactions. The model relates the *b* parameter to large-scale motions and the product *bc* to the small-scale modes. Experimental support for the model has been given by dielectric spectroscopy techniques.[19]

The aim of the present paper is twofold. On the one hand, we use dielectric spectroscopy to follow, in real time, phase separation and crystallization processes of a selected poly(ester–carbonate) block copolymer. On the other, we study the effect of crystallinity, as revealed by X-ray scattering, on the dynamics of the remaining amorphous phase of the block copolymer as crystallization proceeds. The final objective is to correlate the variation of real-time X-ray parameters with the variation of the dielectric permittivity.

2. Experimental Section

2.1. Sample Preparation. A poly(ester–carbonate) copolymer of poly(butylene terephthalate) (PBT) and aliphatic polycarbonate (PC) in a PBT/PC weight relation of 60/40 was investigated in the present paper (see Figure 1). PBT–PC is a family of block copolymers in which the variation of the PBT/PC ratio modifies substantially the melting point and less effectively the glass transition temperature.[9] For the synthesis of the copolymer a three-stage polycondensation method was used as described elsewhere.[9,11] Samples were prepared by compression molding between thin Teflon films at a temperature 20 °C above the melting point ($T_m \approx 100$ °C). Films with a thickness of approximately 300 μm were subsequently quenched at room temperature. Calorimetric measurements were carried out using a Perkin-Elmer DSC-4 scanning calorimeter. Calibration was made by using an indium standard.

2.2. Techniques. Dielectric permittivity ($\epsilon^* = \epsilon' - i\epsilon''$) measurements were performed in the frequency range 10^3–10^6 Hz by using a Hewlett-Packard HP 4192A impedance analyzer. Films 300 μm in thickness were provided with circular gold electrodes 4 cm in diameter by sputtering. The films were placed between two gold-plated stainless steel electrodes. The dielectric cell was introduced in a homemade cryostat operating in a temperature-controlled nitrogen atmosphere. The temperature error during the measuring time was estimated to be ±0.1 °C. The measuring time involved in a sweep from 10^3 to 10^6 Hz is about 34 s. This gives an error in the crystallization time of ±0.3 min. To carry out measurements in amorphous specimens, the sample was heated above the melting point. The high viscosity of the sample allowed us to keep the electrode geometry without appreciable changes during measurements. The sample was subsequently quenched at room temperature in the amorphous state by cooling the film between two metallic blocks.

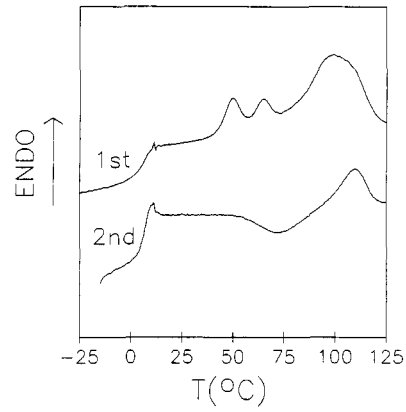

Figure 2. First- and second-run DSC traces for the PBT–PC(60/40) block copolymer. Heating rate = 20 °C/min.

Wide- and small-angle X-ray scattering (WAXS and SAXS) experiments were performed using a double-focusing mirror monochromator on the polymer beam line at HASYLAB (Hamburg, Germany). The samples were heated in vacuum (10^{-2} Torr). Thermal contact and homogeneous heating were ensured by a thin aluminum foil covering the surfaces of the film. The wavelength used was 0.15 nm. After reaching the selected crystallization temperature T_c, scattering patterns were recorded at selected accumulation times using a linear position-sensitive detector and corrected for fluctuations in the intensity of the primary beam and background. The data acquisition system is based on CAMAC hardware and modulator software.[20]

3. Results

3.1. Thermal Behavior. PBT–PC(60/40) samples stored at room temperature for a long time exhibit a glass transition temperature at about 3.5 ± 2.5 °C followed by several endothermic peaks as revealed by the DSC first-run scan shown in Figure 2. After cooling at 20 °C/min, the second heating run reveals, in addition to the steplike glass transition, one crystallization exothermic peak followed by the corresponding melting peak. This experiment indicates that upon cooling from the melt an amorphous polymer is obtained.

Parts a and b of Figure 3 show the temperature dependence of the WAXS and SAXS patterns using the same heating rate as in the DSC experiments. At low temperatures the WAXS patterns show the existence of incipient Bragg maxima superimposed on an amorphous halo centered around 15 ± 0.25 nm^{-1} in the investigated angular range. The position of the Bragg maxima (q = 12.3, 14.7, and 16.7 ± 0.25 nm^{-1}) correspond to the reported α crystal phase of the PBT homopolymer.[5] At temperatures in the region of the higher temperature DSC endothermic peak (see Figure 2), the Bragg maxima disappear, suggesting the melting of the crystalline domains. In the temperature region corresponding to the intermediate endotherms ($T \approx 60$ °C) no changes in the diffraction pattern are observed. The corresponding SAXS pattern at room temperature exhibits the existence of a broad maximum centered at about 0.5 ± 0.016 nm^{-1}. As temperature increases, the maximum shifts toward lower q values and finally it disappears at about 100 °C. Figure 4 shows the variation of q_{max} as a function of temperature, indicating first a constancy of $q_{max} = 0.5$ nm^{-1} up to ≈50 °C and then a decrease of q_{max} down to $q_{max} \approx 0.29$ nm^{-1} for $T \approx 100$ °C.

3.2. Real-Time X-ray Scattering during Crystallization. Parts a and b of Figure 5 show the variation of the wide- and small-angle X-ray scattering patterns,

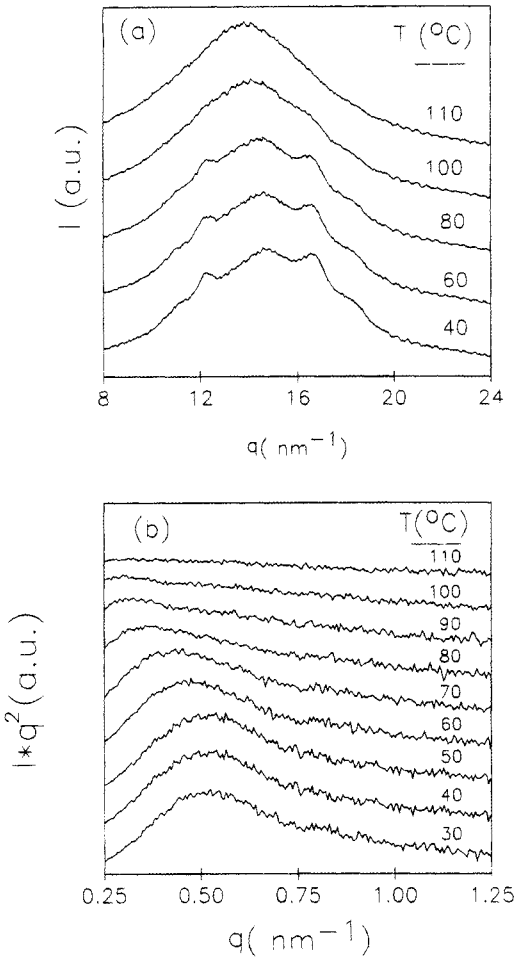

Figure 3. WAXS (a) and SAXS (b) as a function of $\mathbf{q} = (4\pi \sin \theta)/\lambda$ at different temperatures taken at 20 °C/min. The patterns have been shifted along the vertical direction for clarity.

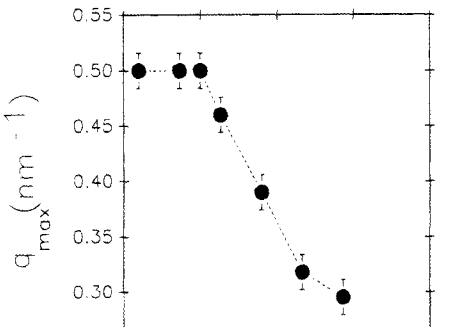

Figure 4. Plot of q_{max} from SAXS as a function of temperature. Heating rate = 20 °C/min.

respectively, as a function of crystallization time. The patterns were obtained in real time (accumulation time of 60 s for WAXS and 20 s for SAXS) during an isothermal crystallization process of the copolymer at $T_c = 31 \pm 0.5$ °C. As crystallization time increases, Bragg reflections appear in the WAXS patterns corresponding to the α-crystalline structure of PBT.[5,21]

The initial SAXS pattern (Figure 5b) indicates the existence of a long spacing of about $L \approx 13.6$ nm already present in the early stages of the isothermal crystallization at $T_c = 31$ °C ($t < 9$ min). The value of the q vector remains constant up to about 250 s (Figure 6a).

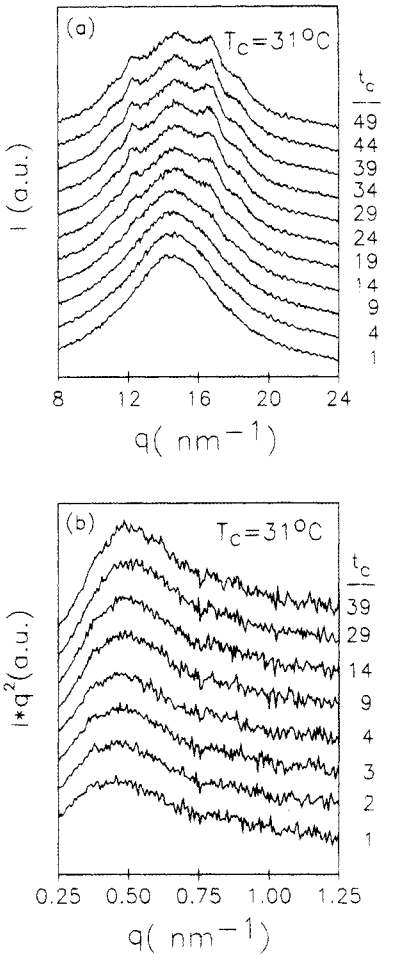

Figure 5. WAXS (a) and SAXS (b) patterns of the PBT–PC-(60/40) block copolymer as a function of $\mathbf{q} = (4\pi \sin \theta)/\lambda$ at selected crystallization times (min) at $T = 31$ °C.

At longer times it bends upward and finally reaches a plateau for longer times ($t > 2000$ s). On the contrary, the intensity of the scattering maximum increases logarithmically with time for the early stages and levels off for times $t > 2000$ s (Figure 6b).

3.3. Dielectric Relaxation of the Amorphous and Semicrystalline Polymer. Dielectric loss (ϵ'') and dielectric constant (ϵ') values measured as a function of the temperature at 10^3 Hz for the amorphous and semicrystalline samples are illustrated in parts a and b of Figure 7, respectively. The semicrystalline sample is the result of keeping the amorphous sample at $T = 31$ °C for several hours to allow the development of crystallinity. Two main dielectric relaxations can be distinguished in the temperature range investigated: the β and the γ relaxations in the order of decreasing temperature according to the criteria followed for similar poly(ether–ester) block copolymers.[11,22] The ϵ'' intensity of the β relaxation process is dramatically affected by the presence of crystallinity (Figure 7). On the other hand, the γ relaxation process remains nearly unaffected during crystallization.

According to the DSC results, the β relaxation can be attributed to the large-scale motions which appear above the glass transition temperature. In amorphous polymers, β and α are used to designate local and long-range relaxation processes, respectively. However, in the field of thermoplastic elastomers γ and β are referred to as the fast (local) and slow (long range) relaxation processes, respectively.[5,22–24] In the present

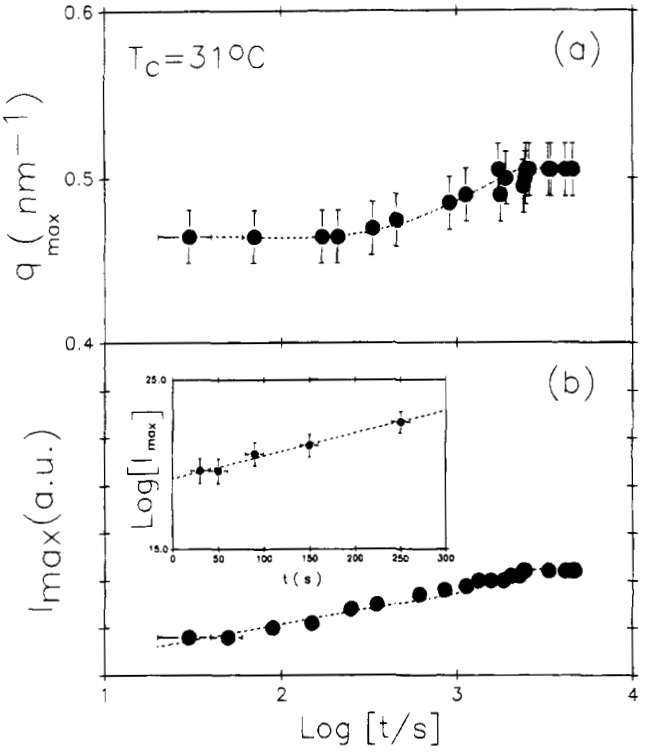

Figure 6. Plot of q_{max} (a) and I_{max} (b) as a function of time at T = 31 °C.

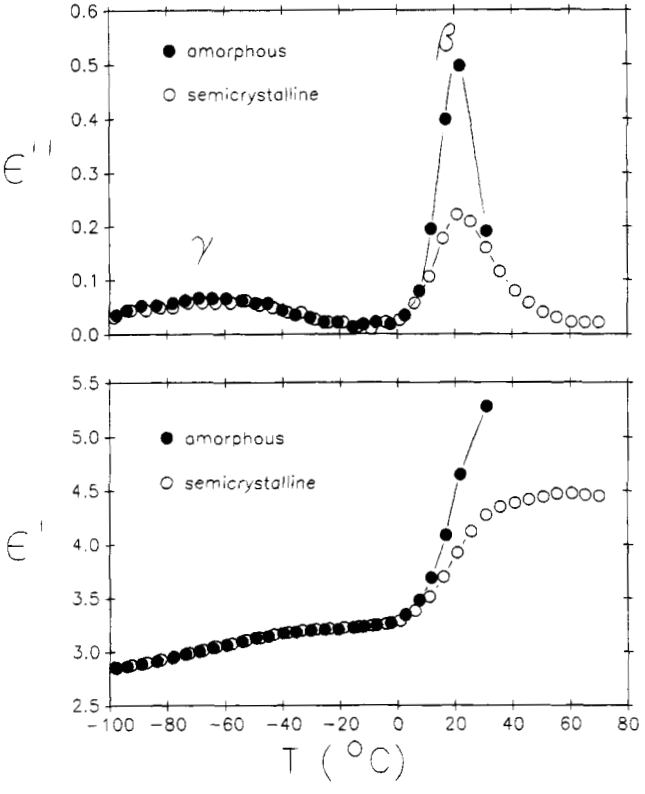

Figure 7. (a) ϵ'' and (b) ϵ' for the amorphous (●) and semicrystalline (○) samples as a function of temperature at 10^3 Hz.

study we shall use the latter terminology. The β process, in the semicrystalline sample, exhibits a Vogel–Fulcher–Tamann type temperature dependence as previously reported.[11] The intensity of the β relaxation is higher in the amorphous sample than in the semicrystalline one, in accordance with other polymeric systems.[13–15,25]

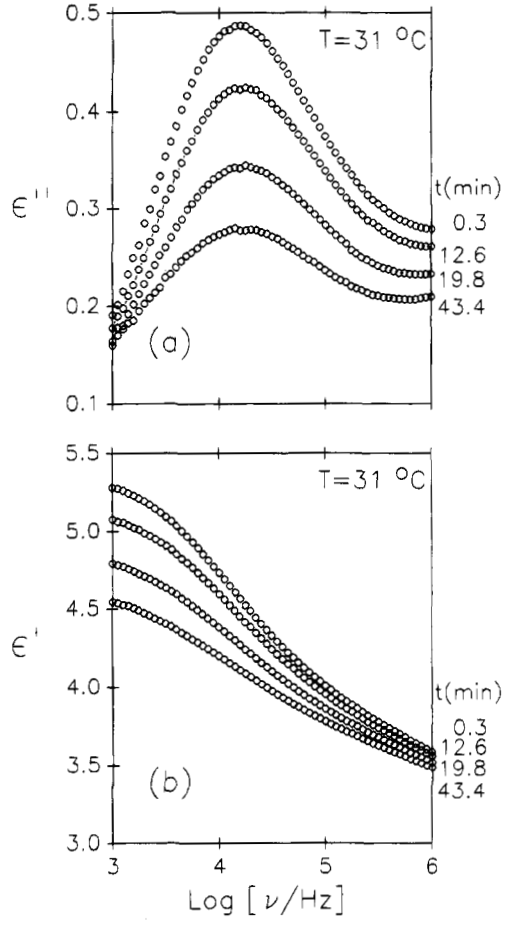

Figure 8. Real-time evolution of the β relaxation dielectric loss, ϵ'' (a) and ϵ' (b), values versus frequency and crystallization time during an isothermal crystallization process at T = 31 ± 0.5 °C.

Subglass relaxation processes are commonly associated with local motions of dipolar groups attached to the polymeric chain. In PBT the γ relaxation has been related to the motions of the ester groups attached to both sides of the phenylene ring.[22] In PBT–PO4 copolymers the γ process is expected to be a combination of local mode motions of both the ether groups present in the soft-segment units and the ester moiety of the PBT segments. In the case of polycarbonates the γ process is associated with local motions of the carbonate groups.[26] In our case, PBT–PC(60/40), the γ process is expected to be mainly due to the contribution of the ester groups from hard PBT segments and of the carbonate groups from the soft PC segments both in the amorphous phase.

3.4. Real-Time Variation of the β Relaxation Process upon Crystallization. Figure 8 shows the real-time evolution of the β relaxation during an isothermal crystallization process at T_c = 31 ± 0.5 °C for the investigated block copolymer. Every single curve represents the dependence of ϵ'' and ϵ' versus frequency at a selected crystallization time. As crystallization time increases, a reduction of the intensity of the β relaxation process is observed. On the contrary, the frequency of the maximum loss remains almost constant. Figure 9 shows the variation of the logarithm of the maximum loss frequency, ν_{max}, and of the relative variation of the dielectric loss value at the maximum as a function of the crystallization time. If one considers that $(2\pi\nu_{max})^{-1}$ is an average relaxation time,[25] the observed constancy of ν_{max} suggests that the overall

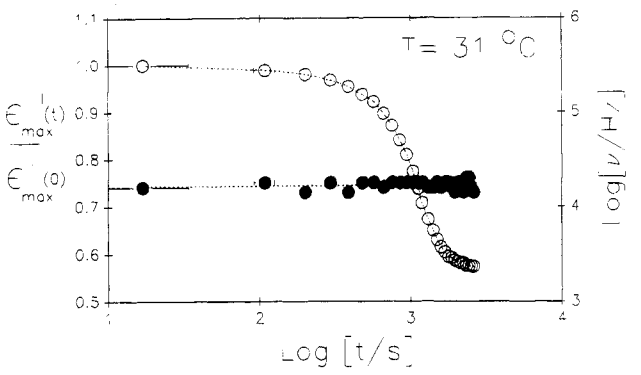

Figure 9. Variation of the frequency of maximum loss values, ν_{max} (●), and relative dielectric loss, $\epsilon''_{max}(t)/\epsilon''_{max}(0)$ (○), as a function of crystallization time (t) for the isothermal crystallization at T = 31 °C.

chain mobility in the remaining amorphous phase is almost unaffected by the crystallization process.

3.5. Phenomenological Analysis of the Experimental Results. In order to quantify the ϵ^* variation as derived from Figures 8a and 8b, during the crystallization process, a fitting of the experimental curves by means of eqs 1 and 2 has been attempted by considering the β and the γ relaxations as the slow and fast processes, respectively. Our frequency range does not cover the complete γ relaxation process for the crystallization temperature of interest. Therefore, we have simulated the γ relaxation process by the extrapolation procedure of Coburn and Boyd.[15] This procedure was performed for the initial amorphous sample and for the same sample after crystallization. The results are shown in the Appendix. In this way the parameters of the γ process can be directly obtained for the initial and final crystallization times. For the intermediate crystallization times, the fitting parameters of the γ process were allowed to vary between the limiting obtained values.

Figure 10 shows the change of the Cole–Cole plots corresponding to the β and γ relaxations during the crystallization process. The continuous lines correspond to the calculated fittings according to the HN equations (eqs 1 and 2). The parameters calculated in Figure 10 are shown in Table 1. To estimate the accuracy of the fitting parameters, their values have been varied. We found that the maximum possible variation without provoking a significant deviation between the measured and calculated curves presented in Figure 10 was less than ±5% for b, c, and $\Delta\epsilon$ and less than ±10% for τ_0.

4. Discussion

4.1. Structure and Thermal Behavior. Similarly to the case of other hard–soft systems based on PBT, the WAXS pattern (Figure 3a) of the PBT–PC(60/40) block copolymer at $T \leq 80$ °C reveals the existence of a crystalline phase predominantly formed by PBT segments. The alternation of hard-segment crystalline regions with hard–soft amorphous domains gives rise to a difference in electronic density which manifests itself by the appearance of a long spacing in the SAXS pattern (Figure 3b). From the SAXS data at $T \leq 30$ °C (Figure 3b), a long period $L = 12.5 \pm 0.5$ nm is obtained which is comparable to those observed for similar systems.[27,28] As temperature is increased, the melting of the crystalline PBT hard-segment domains is revealed by the disappearance of both the Bragg peaks (Figure 3a) and the long period (Figure 3b) at $T \approx 110$ °C. The

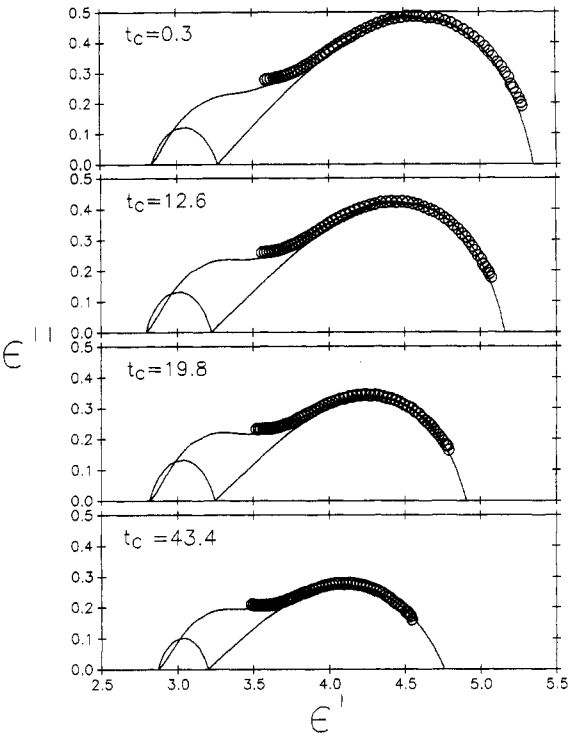

Figure 10. Cole–Cole diagrams of the β and γ relaxations for selected crystallization times (t_c (min)) at $T_c = 31 \pm 0.5$ °C. Solid curves denote best fits calculated according to eqs 1 and 2. Parameters of the fits are shown in Table 1.

Table 1. $\Delta\epsilon_\beta$, b_β, c_β, and τ_{0_β} Obtained from the Fitting of Eqs 1 and 2 during Isothermal Crystallization at T = 31 °C[a]

t (min)	$\Delta\epsilon_\beta$	b_β	c_β	τ_{0_β} (s)	$\Delta\epsilon_\gamma$	b_γ	τ_{0_γ} (s)
0.3	2.08	0.79	0.39	2.8×10^{-5}	0.43	0.65	1.4×10^{-8}
12.6	1.93	0.78	0.36	3.2×10^{-5}	0.43	0.7	1.5×10^{-8}
19.8	1.66	0.70	0.40	3.2×10^{-5}	0.43	0.7	1.5×10^{-8}
43.4	1.56	0.54	0.5	2.6×10^{-5}	0.33	0.69	1.5×10^{-82}

[a] The extrapolated parameters corresponding to the γ process are denoted by $\Delta\epsilon_\gamma$, b_γ, and τ_{0_γ}.

melting of hard segments thus gives rise to the higher temperature endothermic maximum observed by DSC (Figure 2, first run). In an attempt to characterize the degree of crystallinity of the system, the area under the melting endotherm has been measured and normalized by the sample mass. By using 34.63 cal/g[29] as the value for the 100% crystalline PBT, an estimate of the crystallinity of ≈8% can be obtained.

The existence of other endothermic peaks between the glass and melting temperatures shown in Figure 2 has been reported in copoly(ester–ether) systems. These endotherms are dependent on annealing conditions.[5] The origin of these peaks has been attributed to a slow enthalpy relaxation of PBT hard segments placed in the intercrystalline region.[5,30,31] This effect occurs in the temperature region in which the glass transition temperature of semicrystalline PBT ($T_g = 44.5 \pm 7.5$ °C) is observed.[29] The decrease of q_{max} (Figure 4) for temperatures higher than ≈50 °C could be consistent with an expansion of the distance between the gravity centers of the crystalline regions due an enthalpic relaxation of the amorphous phase. However, from the proximity of the melting endotherm one cannot discard the contribution of premelting effects.

The SAXS pattern of the molten state at T = 110 °C exhibits an absence of structure in the q range covered (Figure 3b). Upon quenching at 31 °C the initial WAXS

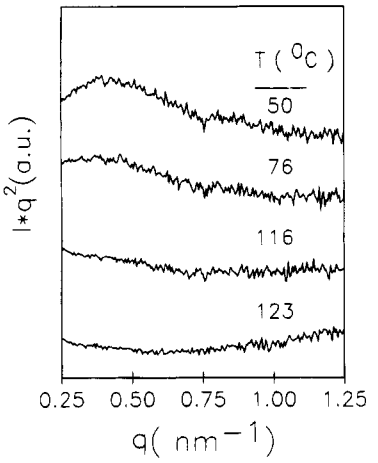

Figure 11. SAXS patterns at different temperatures taken during the cooling process from the melt.

pattern (60 s, Figure 5a) exhibits qualitatively the same features of the pattern in the melt with an absence of Bragg peaks. The corresponding SAXS data (60 s, Figure 5b) show a maximum centered at about $q = 0.46 \pm 0.016$ nm^{-1}. This finding might indicate the occurrence of a significant amount of phase separation, probably achieved during the cooling process. In order to test this conjecture, SAXS patterns at selected temperatures during the cooling process are presented in Figure 11. The relative high cooling rate (≈40 °C/min) and the used accumulation time (20 s) give rise to a high uncertainty in temperature (≈±7 °C). However, from the data obtained, a qualitative discussion is possible. Figure 11 shows that during the cooling process from the melt ($T = 130$ °C) to the temperature of crystallization, a small-angle X-ray maximum appears indicating the occurrence of regions with different electronic densities. It is known that, at equilibrium, the polymeric chains in a diblock copolymer adopt a minimum free energy configuration in which blocks are mixed.[2] In many cases the interaction parameter, χ_{AB}, depends inversely on temperature. Therefore, it is expected that a decrease in temperature will induce an increase in χ_{AB}, which, in turn, will tend to limit the contacts among monomers.[2,3] When the polymerization degree is large enough, this effect produces a local segregation (microphase separation) accomplished by losses of translational and configurational entropy.[2] According to this view, the results shown in Figure 11 could support the concept of a partial microphase separation of the PBT−PC(60/40) blocks upon cooling from the molten state.

4.2. Real-Time Precrystallization Effects. By comparing the time evolution of the WAXS and SAXS scattering patterns during the isothermal crystallization process (Figure 3 and 6), a maximum in the SAXS pattern is already present at very short times ($t < 1$ min) while no traces of crystallinity from WAXS are detected in the same time interval. Furthermore, the position of the SAXS maximum (q_{max}) exhibits no time evolution during the early crystallization stages at $T = 31$ °C ($t < 250$ s) while the intensity of the maximum (I_{max}) shows an exponential increase as a function of time for $t < 250$ s as shown in the inset of Figure 6b. These observations are in line with the recent findings of Imai et al. concerning the crystallization of poly(ethylene terephthalate) (PET) from the glassy state.[32-34] These authors found for PET the existence of an induction period prior to crystallization where a phase separation process takes place. The phase separation

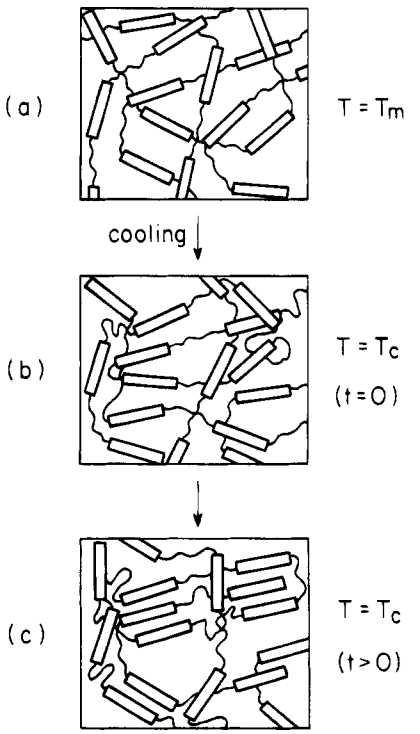

Figure 12. Schematics of the phase separation (b) and crystallization process (c) of the PBT thermoplastic elastomer from the molten state (a). Rectangular boxes and lines represent hard and soft segments, respectively. For the sake of simplicity, chain folding of PBT segments has not been drawn.

process has been analyzed, in the early stages of phase separation, in light of the Cahn linearized theory for spinodal decomposition.[33,35] A similar approach has been followed by Okamoto et al. to interpret the phase separation mechanism in a PBT−Bisphenol A polycarbonate copolymer.[36]

With these ideas in mind, we can attempt to interpret our results in the following way. Upon cooling, a phase separation process takes place, provoking the appearance of a long period of about 13.6 nm. During the isothermal treatment at $T = 31$ °C an induction period exists ($t < 250$ s) where microphase separation further proceeds as revealed by the invariance of q_{max} and the concurrent exponential increment of I_{max} (inset Figure 6b). According to the linearized Cahn theory for spinodal decomposition, the variation of the scattering intensity is given by

$$I_{max}(q,t) = I(q_{max},0) \exp(2R(q_{max})t) \qquad (3)$$

where $R(q)$ is the growth rate of the density fluctuation. The application of eq 3 to our case gives rise to a value for $R(q_{max})$ of 3×10^{-4} s^{-1}, which is comparable with the value calculated for PET.[33]

For crystallization times $t > 250$ s, crystallization starts, as revealed by the appearance of incipient Bragg peaks in the WAXS pattern for times longer than 500 s. The onset of crystallization provokes a shift of q_{max} toward higher values. For $t > 2000$ s crystallization rate decreases dramatically, provoking the simultaneous leveling off observed for q_{max} and I_{max}.

Figure 12 schematically offers an idealized view of the phase separation and final crystallization process according to the above-mentioned features. In our case, during the induction period, within the experimental error, no evidence for any shift in q_{max} toward smaller

values is observed, in contrast with the findings of Imai et al.[34] for the crystallization of PET. Such an effect has been theoretically predicted.[37,38] It has been proposed[39] that competing phenomena may affect the phase separation process. In particular, recent Monte Carlo simulations show that when nearest-neighbor entities interact with two disparate energies, a pinning of the structure factor occurs, arresting the process of domain growth and, consequently, provoking an invariance of q_{max} for times longer than a given one.[40] In our case, one of the blocks forming the copolymer may crystallize (PBT) subsequently to the phase separation process. The formation of regions where a parallel alignment of PBT segments exists is expected. These localized regions may act as cross-links stabilizing the region which is undergoing phase separation. Such an effect has been observed in gelation experiments where the occurrence of cross-linking arrests the growth of the separated domains.[41,42]

4.3. Influence of the Crystalline Material on the Dynamics of the Amorphous Phase during Crystallization. A particularly interesting result is the decrease of the dielectric strength of about 25% of its initial value after a crystallization time of 43 min (Table 1). Since $\Delta\epsilon$ is proportional to the density of dipoles involved in the relaxation process,[25,26] the decrease of $\Delta\epsilon$ with t can be associated with the progressive reduction of the amorphous phase as hard segments crystallize. The observed reduction of $\Delta\epsilon$ is larger than the decrease of amorphous material as derived from DSC crystallinity. the enhanced reduction of $\Delta\epsilon$ with increasing crystallinity has been previously reported in different polymers.[25,29,43,44] From this result one may infer, in agreement with other authors, the existence of a tightly bound amorphous phase which appears as a consequence of constraints of these rigid amorphous chains provoked by the influence of the crystal lamellae.

It is known that crystallization hinders the overall mobility of chain segments in the amorphous phase anchored to the crystals.[15] The presence of crystals seem to affect more likely large-scale, rather than small-scale, motions. In particular, polymers like PET and PEKK which crystallize by formation of spherulites exhibit a shift of the frequency of maximum loss of the relaxation process appearing above T_g.[13-15,25]

The observed invariance of ν_{max} for the PBT−PC(60/40) block copolymer during the isothermal treatment (Figure 8) can be understood by considering the morphology of this type of block copolymer. Typically, thermoplastic elastomers based on PBT can build up chain-folded lamellae of the crystallizable hard segments[28,45] embedded on an amorphous phase consisting of a mixture of soft and uncrystallized hard segments. On a larger scale, crystalline lamellae arrange themselves on spherulitic structures.[46] The relation of PBT crystallized material to the overall spherulite volume is smaller than for typical spherulites of homopolymers due to the existence of the soft-segment moieties. The amorphous phase, consisting of a mixture of both soft and hard components, is expected to be less constrained by the crystalline lamellae than when they arrange within more compact spherulitic superstructures like those formed by homopolymers. This explanation can account for the observed invariance of ν_{max} for the PBT−PC(60/40) block copolymer. This conclusion is further supported by the evolution of the β relaxation, as analyzed by the HN approach, during the isothermal crystallization process. For the first stages of isothermal crystallization the β process is strongly asymmetric, as deduced from the c initial value. As crystallinity develops, the relaxation curve becomes slightly broader and more symmetric, as revealed by the concurrent decrease of b and increase of the c values, respectively. According to the predictions of the Sch model, a decrease of b can be interpreted as due to the increasing hindrance of the large-scale motions as crystallization proceeds. On the other hand, the value of the product cb is related to small-scale motions which are less affected by the crystallization process. It is noteworthy that the variation of the b and c parameters observed in our case (Table 1) is smaller than that observed in other polymers like PET[13] and PEKK[14] although they exhibit a comparable decrease of $\Delta\epsilon$ on crystallization. This result suggests that the morphological arrangement typical of PBT thermoplastic elastomers has less influence on the dynamics of the amorphous phase than the spherulitic morphology characteristic of homopolymers.

5. Conclusions

Dielectric relaxation and X-ray scattering measurements in real time have been used to monitor and characterize the changes occurring in a hard−soft block copolymer during crystallization. The changes observed have been interpreted as follows. (1) Upon cooling from the melt, microphase separation occurs, giving rise to the appearance of a long spacing, which suggests the appearance of domains with a slight difference in electronic density. (2) In the early stages of isothermal crystallization, the microphase separation process follows the linearized Cahn theory for spinodal decomposition. (3) Crystallization of the PBT hard segments takes place in the hard segment rich domains. This finding is supported by the invariance of the frequency of maximum loss during the crystallization process. (4) The changes occurring in the dielectric relaxation process during the isothermal treatment are phenomenlogically described in terms of the Havriliak−Negami formulation. The β-relaxation broadens and becomes more symmetric as crystallization proceeds. This evolution is interpreted, according to the Sch model, by the restriction of the long-scale motions of the polymeric chains as the material is filled in with crystals. (5) The influence of crystalline lamellae on the dynamics of the amorphous phase is smaller for the investigated block copolymer than for other homopolymers. This is suggested to be due to the fact that PBT thermoplastic elastomers crystallize in the form of spherulites with an enhanced amount of amorphous phase as compared with that of the related hompolymers.

Acknowledgment. The authors are indebted to the CICYT (Grant MAT 94-0740E), Spain, for generous support of this investigation. Z.R. thanks the Tempus Program (JEP 0644) and NATO for the tenure of grants to support his investigations. Measurements of HASYLAB (Hamburg, Germany) were funded by the program Human Capital and Mobility, Access to Large Installations EC.

Appendix

The extrapolation procedure of Coburn and Boyd[15] assumes the parameters describing the fast relaxation process ($\Delta\epsilon_\gamma$, b_γ) to be linear functions of the temperature. The procedure was applied by carrying out the following steps:

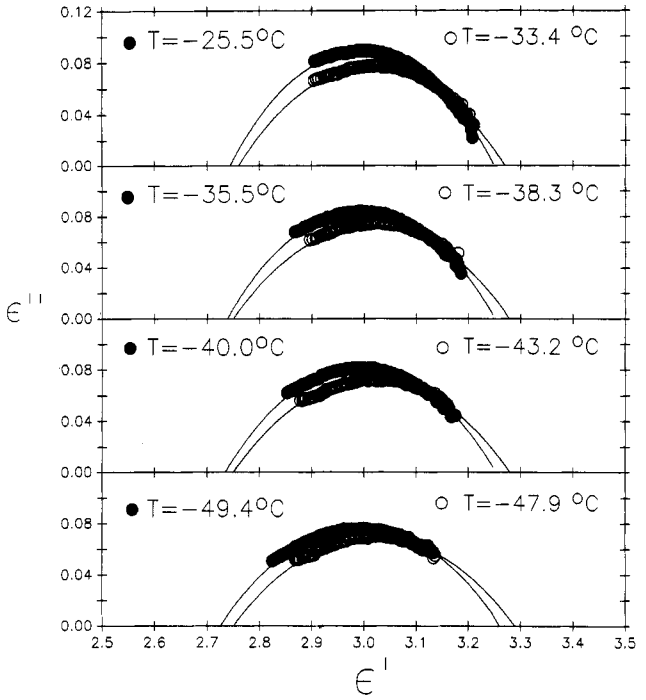

Figure 13. Plot of ϵ'' versus ϵ' for the amorphous (●) and semicrystalline (○) samples at different temperatures.

Table 2. b_γ, $\Delta\epsilon_\gamma$, and τ_{0_γ} Obtained from the Fitting of Eq 2 in the Case of the γ Relaxation Process of the Amorphous Sample at Selected Temperatures

T (°C)	$\Delta\epsilon_\gamma$	b_γ	τ_{0_γ}
−49.4	0.53	0.35	8.8×10^{-6}
−40.0	0.52	0.38	3.1×10^{-6}
−35.5	0.51	0.40	2.0×10^{-6}
−25.5	0.50	0.43	8.2×10^{-7}

(a) The parameters describing the γ process, ϵ_{0_γ}, ϵ_{∞_γ}, τ_{0_γ}, and b_γ, were determined in the temperature range between −50 and −20 °C where the γ process appears in the frequency range covered by our measurements.

(b) Since our frequency range does not cover the region where the γ relaxation process appears at high temperature, the corresponding parameters at such high temperatures were extrapolated from the data at low temperatures by assuming that $\Delta\epsilon_\gamma$ and b_γ are linear functions of the temperature and that τ_{0_γ} follows an Arrhenius behavior.

(c) The parameters $\Delta\epsilon$, τ_0, b, and c for the β process were determined by fitting the calculated curve for the total process to the measured values under the condition that $\epsilon_{0_\gamma} = \epsilon_{\infty_\beta}$. These values are denoted by $\Delta\epsilon_\beta$, τ_{0_β}, b_β, and c_β.

A subroutine based on the Newton method[47] was used in the fitting. Figure 13 shows Cole–Cole plots representing ϵ'' as a function of ϵ' at two pairs of selected temperatures in the range where the γ relaxation maximum appears for both the amorphous and the semicrystalline copolymer. A fitting of the experimental curves by means of eqs 1 and 2 has been attempted assuming $c = 1$. The solid lines in Figure 13 represent the best calculated fittings obtained. The corresponding parameters, denoted by $\Delta\epsilon_\gamma$, b_γ, and τ_{0_γ}, are shown in Tables 2 and 3 for the amorphous and semicrystalline samples, respectively. Figure 14 and 15 show these parameters as a function of temperature. The extrapolated values at 31 °C are also shown. As one can see, the observed subglass processes (γ) can be described satisfactorily by assuming a symmetric broadening (c = 1). In accordance with the isochronal results (Figure 7) the γ process is slightly affected by the presence of crystals.

Table 3. b_γ, $\Delta\epsilon_\gamma$, and τ_{0_γ} Obtained from the Fitting of Eq 2 in the Case of the γ Relaxation Process of the Semicrystalline Sample at Different Temperatures

T (°C)	$\Delta\epsilon_\gamma$	b_γ	τ_{0_γ}
−47.9	0.54	0.32	1.1×10^{-5}
−43.2	0.53	0.34	6.5×10^{-6}
−38.3	0.51	0.36	3.7×10^{-6}
−33.4	0.51	0.37	2.2×10^{-6}

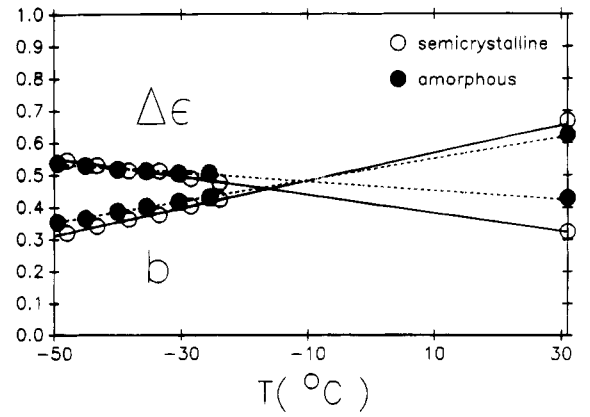

Figure 14. Plot of $\Delta\epsilon_\gamma$ and b_γ for the amorphous (●) and semicrystalline (○) samples as a function of temperature. Extrapolated values at 31 °C are also shown.

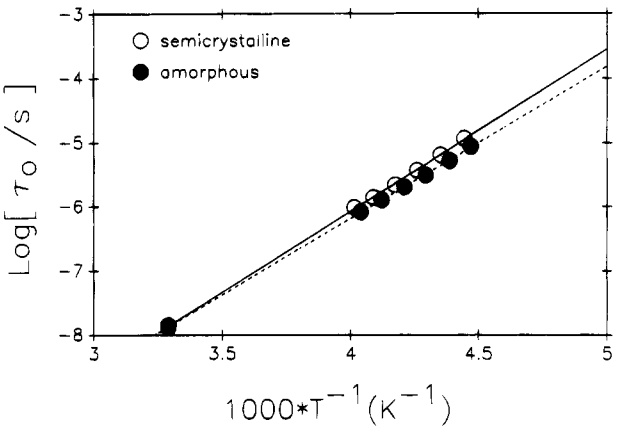

Figure 15. Plot of log τ_{0_γ} versus reciprocal temperature for the amorphous (●) and semicrystalline (○) samples. Extrapolated values at 31 °C are shown.

References and Notes

(1) *Thermoplastic Elastomers, A Comprehensive Review*; Lesse, N. R., Holden, G., Schroeder, H. E., Eds.; Hanser Publishers: Munich, 1987.
(2) Bates, F. S.; Fredrickson, G. H. *Annu. Rev. Phys. Chem.* **1990**, *41*, 525.
(3) Floudas, G.; Pakula, T.; Fischer, E. W.; Hadjichristidis, N.; Pispas, S. *Acta Polym.* **1994**, *45*, 176.
(4) Tanaka, H.; Nishi, T. *Phys. Rev. Lett.* **1985**, *55*, 1102.
(5) Castles, J. L.; Vallance, M. A.; McKenna, J. M.; Cooper, S. L. *J. Polym. Sci., Polym. Phys. Ed.* **1985**, *23*, 2119.
(6) Roslaniec, Z. *Polymer* **1992**, *33*, 1717.
(7) Roslaniec, Z. *Polymer* **1993**, *34*, 1249.
(8) Roslaniec, Z. *Polymer* **1993**, *34*, 359.
(9) Roslaniec, Z.; Wojcikiewicz, H. *Polimery* **1988**, *33*, 360.
(10) Roslaniec, Z. *Polymery* **1992**, *37*, 328.
(11) Roslaniec, Z.; Ezquerra, T. A.; Baltá-Calleja, F. J. *Colloid Polym. Sci.* **1995**, *273*, 58.
(12) Williams, G. In *Materials Science and Technology: Structure and Properties of Polymers*; Cahn, R. W., Haasen, P., Kramer, E. J., Eds.; VCH: Weinheim, 1993.

(13) Ezquerra, T.A.; Baltá-Calleja, F. J.; Zachmann, H. G. *Polymer* **1994**, *35*, 2600.
(14) Ezquerra, T. A.; Majszczyk, J.; Baltà-Calleja, F. J.; López-Cabarcos, E.; Gardner, K. H.; Hsiao, B. S. *Phys. Rev. B* **1994**, *50*, 6023.
(15) Coburn, J. C.; Boyd, R. H. *Macromolecules* **1986**, *19*, 2238.
(16) Havriliak, S.; Negami, S. *Polymer* **1967**, *8*, 161.
(17) Colmenero, J.; Alegria, A.; Alberdi, J. M.; Alvarez, F. *Phys. Rev. B* **1991**, *44*, 7321.
(18) Schönhals, A.; Schlosser, E. *Colloid Polym. Sci.* **1989**, *267*, 125.
(19) Schönhals, A.; Kremer, F.; Schlosser, E. *Phys. Rev. Lett.* **1991**, *67*, 999.
(20) Boulin, C.; Kempf, R.; Koch, M. H. J.; Mclaughlin, S. M. *Nucl. Instrum. Meth. Phys. Res. (A)* **1986**, *249*, 399.
(21) Wings, N.; Trafara, G. *Angew. Makromol. Chem.* **1994**, *217*, 91.
(22) Gallagher, K. P.; Zhang, X.; Runt, J. P.; Huynh-ba, G.; Lin, J. S. *Macromolecules* **1993**, *26*, 588.
(23) Runt, J.; Martynowicz, L. M.; Brezny, D. M.; Mayo, M. *Macromolecules* **1989**, *22*, 3908.
(24) North, A. M.; Pethrick, R. A.; Wilson, A. D. *Polymer* **1978**, *19*, 923.
(25) Williams, G. *Adv. Polym. Sci.* **1979**, *33*, 59.
(26) Hedvig, P. *Dielectric Spectroscopy of Polymers*; Adam Hilger Ltd.: Bristol, 1977.
(27) Castles-Stevenson, J.; Cooper, S. L. *Macromolecules* **1988**, *21*, 1309.
(28) Fakirov, S.; Apostolov, A.; Boeseke, P.; Zachmann, H. G. *J. Macromol. Sci., Phys.* **1990**, *B29* (4), 379.
(29) Cheng, S. Z. D.; Pan, R.; Wunderlich, B. *Makromol. Chem.* **1988**, *189*, 2443.
(30) Stevenson, J. C.; Cooper, S. L. *J. Polym. Sci., Polym. Phys. Ed.* **1988**, *26*, 953.
(31) Stevenson, J. C.; Cooper, S. L. *Macromolecules* **1988**, *21*, 1309.
(32) Imai, M.; Mori, K.; Mizukami, T.; Kaji, K.; Kanaya, T. *Polymer* **1992**, *33*, 4451.
(33) Imai, M.; Mori, K.; Mizukami, T.; Kaji, K.; Kanaya, T. *Polymer* **1991**, *33*, 4457.
(34) Imai, M.; Kaji, K.; Kanaya, T. *Phys. Rev. Lett.* **1993**, *71*, 4162.
(35) Cahn, J. W. *J. Chem. Phys.* **1965**, *42*, 93.
(36) Okamoto, M.; Inoue, T. *Polymer* **1994**, *35*, 257.
(37) Furukawa, H. *Adv. Phys.* **1985**, *34*, 703.
(38) Binder, K.; Stauffer, D. *Phys. Rev. Lett.* **1973**, *33*, 1006.
(39) Glotzer, S. G.; Gyure, M. F.; Sciortino, F.; Coniglio, A.; Stanley, H. E. *Phys. Rev. Lett.* **1993**, *70*, 3275.
(40) Glotzer, S. C.; Gyure, M. F.; Sciortino, F.; Coniglio, A.; Stanley, H. E. *Phys. Rev. E* **1994**, *49*, 247.
(41) Hobbie, E. K.; Bauer, B. J.; Han, C. C. *Phys. Rev. Lett.* **1994**, *72*, 1830.
(42) Bansil, R.; Lal, J.; Carvalho, B. L. *Polymer* **1992**, *33*, 2961.
(43) Huo, P. P.; Cebe, P. *Polymer* **1993**, *34*, 696.
(44) Huo, P. P.; Friler, J. B.; Cebe, P. *Polymer* **1993**, *34*, 4387.
(45) Fakirov, S.; Fakirov, C.; Fischer, E. W.; Stamm, M. *Polymer* **1991**, *32*, 1173.
(46) Seymour, R. W.; Overton, J. R.; Corley, L. S. *Macromolecules* **1975**, *8*, 331.
(47) Ebert, K.; Ederer, H.; Isenhour, T. L. *Computer Applications in Chemistry*; VCH: Weinheim, 1989.

MA950164D